# Polymer Diffusion and Mechanical Properties of Films Prepared from Crosslinked Latex Particles

Patrick Pinenq[†] and Mitchell A. Winnik[*,**]—University of Toronto[*]
Benoit Ernst and Didier Juhué[††]—ELF-Atochem CERDATO[††]

*We describe energy transfer (ET) measurements to follow polymer diffusion, as well as oscillatory dynamic mechanical measurements and tensile measurements, on films prepared from structured and unstructured latex particles consisting of a copolymer of butyl methacrylate and butyl acrylate with a $T_g$ of 20 °C. Structure was introduced in the form of a low level (1 mol%) of crosslinking, using seeded semi-continuous emulsion polymerization to control the locus of the crosslinking agent in the particles. Linear dynamic mechanical measurements showed the G′ and G″ were sensitive to the particle morphology, with particular sensitivity exhibited by the elastic modulus G′. The tensile properties were less sensitive to particle morphology; sufficient polymer diffusion occurs during film formation for the films to acquire strength and toughness. As expected, crosslinking increases strength but decreases elongation to break. Some interesting compromises could be found through control of the location of the crosslinked regions of the film.*

## INTRODUCTION

This paper describes factors affecting polymer diffusion in films prepared from aqueous dispersions of partially crosslinked latex particles. Since the latex microspheres are prepared by emulsion polymerization, they are often referred to as emulsion polymers. These emulsion polymers are used for a variety of applications that require the formation of a continuous film with good cohesive properties. These applications include water-based adhesives, paints, and other waterborne coatings. In all of these technologies, the aqueous dispersion is coated onto a solid substrate and allowed to dry, typically at a temperature above the minimum film forming temperature of the particles. As the dispersion dries, the particles come into contact and deform into a void-free film consisting of close-packed polyhedral cells. The interdiffusion of polymer molecules across the boundary between adjacent cells is one of the keys to obtain a film with good cohesive strength.[1-3] In some of these technologies, crosslinking is used to improve the mechanical properties of the coating, particularly its toughness and solvent resistance. Crosslinks can be formed after the coating is applied to the substrate (post-application cure), or a small degree of crosslinking can be introduced into the latex during the particle synthesis. In the latter case, one imagines that much of the mechanical strength of the film results from trans-boundary diffusion of long dangling ends of the crosslinked network.[4]

While thermoset latex systems have a long history, our understanding of the factors affecting their properties remains poor. This situation is beginning to change. Concern for the environment has stimulated an interest in films formed from soft latex particles that cure at room temperature.[5,6] In the absence of crosslinking, these films would be tacky to the touch and have poor abrasion resistance. One of the most important contributions to our current understanding of thermoset latex films is a recent paper by Zosel and Ley,[7] who compared the tensile strength of latex films formed from crosslinked poly(butyl methacrylate) (PBMA) latex with that of films formed from PBMA latex containing linear polymer. In the latter case, the newly formed films were brittle, but these evolved upon annealing at elevated temperature to form mechanically tough films. In contrast, films prepared from latex particles composed of butyl methacrylate (BMA) copolymerized with 2 mol% methallyl methacrylate, which crosslinked during synthesis, remained

[†]Dept. of Chemistry, 80 St. George St., Toronto, Ont., Canada M5S 3H6.
Permanent address: ELF-Atochem, Centre d'Applications de Levallois, 95 rue Danton, F-92300 Levallois-Perret, France.
[*]Author to whom correspondence should be addressed. E-mail: mwinnik@chem.utoronto.ca.
[††]F-27470 Serquigny, France.

brittle even after extensive annealing at high temperature. From these results, one draws the important conclusion that in thermoset latex films, polymer diffusion across the intercellular boundary must precede cure or the films will remain weak. If crosslinking is confined to individual cells, each cell remains an individual microgel with little adhesion to its neighboring cells. In this paper we show that useful films can be prepared from crosslinked latex dispersions if the extent of crosslinking is kept small. At the same time, the extent of crosslinking is sufficient to modify the mechanical properties of the film. We are interested in exploring how these properties change if one could prepare structured latex in which only part of the particle contains a crosslinked polymer. From this perspective, one can imagine the following four limiting scenarios to form the basis of this comparison.

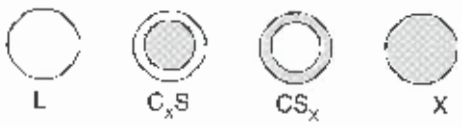


At one limit, (L) is the system consisting of a linear, uncrosslinked latex. At the other limit, (X) is a fully crosslinked latex prepared from a monomer plus a small amount (here 1 mol%) of difunctional crosslinking agent. There are two other limiting cases between these extremes. In $C_xS$ the core of the particle is crosslinked ("core-crosslinked" latex). This type of particle is relatively straightforward to prepare by a three-stage emulsion polymerization reaction in which the seed and second stage polymer contain the crosslinked polymer. In $CS_x$, the core consists of a linear polymer, but the shell is crosslinked. One can imagine preparing such a system by confining the crosslinking agent to the final stage of a multistage semi-continuous emulsion polymerization. If, however, the core and shell polymer have similar compositions, it is difficult to confine the locus of polymerization to the outer regions of the particle. We will refer to latex particles prepared in this way as "third-stage" crosslinked rather than "shell-crosslinked" latex. In these structured particles, the volume fraction of the crosslinked component in the particles is also an interesting variable. The model systems we examine comprise a series of acrylate latexes, copolymers of BMA, with a small amount of butyl acrylate (BA) to lower the glass transition temperature ($T_g$) of the latex polymer, and ethylene glycol dimethacrylate (EGDMA) as the crosslinking agent.

Since polymers that are part of a crosslinked network cannot undergo translational diffusion, chain interpenetration for network chains is limited to the dangling ends. We examine this aspect of the interdiffusion process by labeling the latex particles with donor (D) or acceptor (A) groups suitable for non-radiative energy transfer experiments.[5-10] We prepared films from a 1:1 mixture of donor- and acceptor-labeled particles that are otherwise similar in size and composition. As the polymer chains or segments from adjacent cells interdiffuse, we detected the extent of interdiffusion by fluorescence decay measurement of the growth in energy transfer in the system.

In this paper, we describe the strategy of our experiments and the synthesis and characterization of the various latex particles prepared. We compare polymer interdiffusion in latex films comprised of uncrosslinked and uniformly crosslinked polymers with a similar composition. These results serve as the basis for understanding dynamic mechanical[11] and tensile experiments[12] on films prepared from these dispersions. Our latex samples form films with a lower $T_g$ than those examined by Zosel and Ley.[7] We show that tough elastomeric films are formed on drying, but that the tensile properties evolve as polymer interdiffusion takes place. We also examine structured latex in which the core, representing either 12 or 50% of the particle volume, is crosslinked. Here, energy

**Table 1—Recipes for the Seed Latex Dispersions**

| Materials (g) | $S_x1$ [a] | S2 [a] | S3 [a] | S4 [b] |
|---|---|---|---|---|
| | | | | 43.8 (S2) |
| BMA | 5.466 | 5.446 | 32.814 | 14.583 |
| BA | 0.534 | 0.534 | 3.208 | 1.426 |
| EGDMA | 0.084 | — | — | |
| Water | 150 | 150 | 900 | 40 |
| KPS | 0.18 | 0.18 | 1.081 | 0.06 |
| SDS | 0.9 | 0.9 | 5.4 | 0.076 |
| $NaHCO_3$ | 0.180 | 0.181 | 1.08 | |
| Diameter (nm) | 29 | - | 37 | 79 |

(a) Prepared by batch emulsion polymerization. All amounts are in grams.
(b) Prepared by semi-continuous emulsion polymerization using the product of S2 as the seed latex.

**Table 2—Recipes for the Preparation of Uncrosslinked Latex Samples**

| Materials [a] | $L^{D/7}$ | $L^{A/7}$ | $L^{D/2}$ | $L^{A/2}$ | $L^{D/1}$ | $L^{A/1}$ |
|---|---|---|---|---|---|---|
| **Step 3: Feed** | | | | | | |
| Seed [b] | 8.25 (S4) | 8.25 (S4) | 8.25 (S4) | 8.27 (S4) | 16.47 [c] | 16.4 [c] |
| BMA | 13.667 | 13.67 | 13.675 | 13.679 | 27.33 | 27.33 |
| BA | 1.339 | 1.333 | 1.338 | 1.334 | 2.667 | 2.665 |
| EGDMA | — | — | — | — | — | — |
| V-Fhe | 0.0217 | — | 0.1 9 | — | 0.432 | — |
| 9-AnMA | — | 0.028 | — | 0.14 | — | 0.559 |
| Water | 30 | 30 | 30 | 30 | 50 | 60 |
| KPS | 0.03 | 0.03 | 0.03 | 0 03 | 0.06 | 0/06 |
| SDS | 0.3 | 0.3 | 0.3 | 0.3 | 0.6 | 0.6 |
| Wt% solids | | | | | 3 .5 | 30.2 |

(a) All amounts are in grams.
(b) Seed analogous to S4, but separate preparation, with d = 79 nm, 18.2 wt% solids.

transfer experiments on films prepared from these latex help characterize the particle morphology, and this morphology in turn has a significant effect on the mechanical properties of the film.

## EXPERIMENTAL

### Materials

As described previously,[13] 9-anthryl methacrylate (AnMA) and 9-vinyl phenanthrene (V-Phe) were synthesized. BMA, BA, and EGDMA (all Aldrich) were distilled under vacuum prior to use. Potassium persulfate (KPS), sodium bicarbonate ($NaHCO_3$), and sodium dodecyl sulfate (SDS, Aldrich) were used as received. Distilled water was further purified through a Millipore Milli-Q™ system.

LATEX PREPARATION: All latexes consist of a copolymer of BMA and BA. The monomer ratio was chosen to yield a copolymer with a $T_g$ around 20°C. When crosslinking was required, 1 mol% of ethylene glycol dimethacrylate was added to the monomer. KPS was used as the radical initiator and SDS was used as the surfactant. All latexes were synthesized by two- or three-step free radical emulsion polymerization. First, latex seeds (ca. 37 nm in diameter) were prepared by batch emulsion. In each of the following steps, the particles were brought to their final size through a semi-continuous emulsion polymerization under monomer-starved conditions. In these steps the aqueous phase (containing KPS and SDS) and the organic phase (the monomers) were added separately to the reactor using two feed pumps. The speed of the pumps was set so that no accumulation of the monomers occurs in the flask in order to avoid any secondary nucleation. Polymerizations were conducted under an $N_2$ atmosphere at 80°C. A summary of the recipes used is presented in *Tables* 1-3.

CLEANING OF THE LATEX PARTICLES: Some latex dispersions were cleaned by ion exchange to remove surfactant and other water-soluble ionic materials. The ion-exchange resin (Bio-Rad AG® 501-X8) was first washed with hot deionized water (> 80°C), methanol, and deionized water before use. Twice the weight of the resin, based upon the weight of solids present in the dispersion to be cleaned, was added to the diluted latex dispersion (solids content about 3 wt%), and then the mixture was stirred at room temperature for about 24 hr. Over this time, the viscosity of the dispersion increased and the dispersion became opalescent, indicating formation of colloidal crystalline domains. The ion-exchange resin was removed by gravity filtration.

### Latex Characterization

Particle size and the size distribution were measured by dynamic light scattering employing a Brookhaven BI-90 Particle Sizer. Molecular weights and molecular weight

**Table 3—Recipes for the Preparation of the Core-Crosslinked Latex Samples**

| Materials | $C^{b}_{x(12)}S$ | $C^{A}_{x(12)}S$ | $(C_{x(12)}S)^{b}$ | $(C_{x(23)}S)^{A}$ | $C^{a}_{x(60)}S$ | $C^{A}_{x(60)}S$ | $(C_{x(60)}S)^{b}$ | $(C_{x(60)}S)^{A}$ |
|---|---|---|---|---|---|---|---|---|
| **Step 2: Feed** | | | | | | | | |
| Seeds ($S_x1$)[a] | 22.2 | 22.2 | 22.2 | 21.8 | 21.8 | 21.8 | -- | — |
| BMA | 7.29 | 7.294 | 7.29 | 7.303 | 30.973 | 30.97 | — | -- |
| BA | 0.714 | 0.713 | 0.718 | 0.722 | 3.036 | 3.036 | -- | — |
| EGDMA | 0.123 | 0.115 | 0.115 | 0.114 | 0.488 | 0.483 | — | -- |
| V-Phe | 0.116 | — | 0.114 | — | 0.498 | — | -- | — |
| 9-AnMA | -- | 0.149 | — | 0.749 | — | 0.64 | — | — |
| Water | 20 | 20 | 20 | 20 | 85 | 85 | -- | — |
| KPS | 0.031 | 0.031 | 0.031 | 0.031 | 0.128 | 0.128 | — | — |
| SDS | 0.039 | 0.038 | 0.038 | 0.038 | 0.16 | 0.161 | — | — |
| **Step 3: Feed** | | | | | | | | |
| Seed[a] | 8.2[b] | 8.1[b] | 18.3[b] | 17.4[b] | 39.6[b] | 42.6[b] | 78.83[b] | 85.1[b] |
| BMA | 13.667 | 13.665 | 27.336 | 27.334 | 9.9839 | 9.885 | 19.674 | 19.676 |
| BA | 1.337 | 1.335 | 2.679 | 2.687 | 0.961 | 0.974 | 1.923 | 1.93 |
| EGDMA | — | — | -- | — | — | — | — | — |
| V-Phe | -- | — | 0.585[c] | — | — | — | 0.314 | — |
| 9-AnMA | — | — | -- | 0.558 | — | — | — | 0.402 |
| Water | — | — | 56 | 56 | 20 | 20 | 40 | 40 |
| KPS | — | — | 0.056 | 0.06 | 0.022 | 0.02 | 0.04 | 0.04 |
| SDS | — | — | 0.56 | 0.561 | 0.199 | 0.2 | 0.4 | 0.4 |
| Water Aq 1 | 15 | 15 | -- | — | — | -- | — | -- |
| NaPS | 0.143 | 0.143 | — | — | -- | — | -- | — |
| SDS | 0.161 | 0.161 | — | — | -- | — | — | -- |
| Water Aq 2 | 15 | 15 | — | — | -- | — | -- | — |
| $NaHSO_3$ | 0.066[f] | 0.065[f] | — | -- | — | — | -- | — |
| $CuSO_4$ EDTA | 0.4 | 0.4 | — | -- | — | — | — | — |
| Wt % solids | -- | — | — | -- | — | — | — | — |

(a) Weight of dispersion of the seed particles. The seed dispersion employed (here $S_x1$) is indicated in parentheses. All amounts are in grams.
(b) Weight of dispersion of the seed particles. Here the seed particles are the products of step 2 of the recipe.
(c) Weight of dispersion of the seed particles. Here the seed particles are the product of step 2 of the recipe for $C^{b}_{x(60)}S$.
(d) Weight of dispersion of the seed particles. Here the seed particles are the product of step 2 of the recipe for $C^{A}_{x(60)}S$.
(e) 9-Phenanthrylmethyl methacrylate was used instead of 9-vinyl phenanthrene.
(f) Third stage polymerization carried out at 22°C with redox initiation. Three pumps were used to deliver the two aqueous solutions (Aq 1, Aq 2) and the monomer simultaneously.

**Table 4—Particle Size and Polymer Molecular Weight of the Latex Particles**

| Latex | Diameter (nm) | $10^{-6}$ $M_w$ | $M_w/M_n$ |
|---|---|---|---|
| Seeds | | | |
| S1 | 29 | | |
| S2 | ? | | |
| S3 | 37 | | |
| S4 | 79 | | |
| Uncrosslinked | | | |
| $L^{D/2}$-Phe | 155 | 4.7 | 5.6 |
| $L^{A/2}$ An | 154 | 5.6 | 3.1 |
| $L^{D/2}$-Phe | 151 | 3 | 3.3 |
| $L^{A/2}$ An | 150 | 3.6 | 3.5 |
| Core-crosslinked (12%) | | | |
| $C^{D}_{x(12)}S$ -Phe | 135 | | |
| $C^{A}_{x(12}S$-An | 131 | | |
| $(C_{x(12}S)^{D}$-Phe | 138 | | |
| $(C_{x(12}S)^{A}$-An | 123 | | |
| Core-crosslinked (50%) | | | |
| $C^{D}_{x(50)}S$ -Phe | 157 | | |
| $C^{A}_{x(50)}S$ -An | 138 | | |
| $(C_{x(50}S)^{D}$ -Phe | 153 | | |
| $(C_{x(50}S)^{A}$-An | 140 | | |
| Shell-crosslinked (50%) | | | |
| $CS_x$ | 146 | | |
| Fully crosslinked | | | |
| $X^{D}$-Phe | 142 | | |
| $X^{A}$-An | 147 | | |
| $X'^{D}$-Phe[a] | 65 | | |
| $X'^{A}$-An[a] | 66 | | |

(a) Stage 2 from the synthesis of $C^{D}_{x(12}S$ -Phe and $C^{A}_{x(12}S$-An, respectively.

distributions of the uncrosslinked latex polymers were determined by gel permeation chromatography (GPC), using two Ultrastyragel columns ($500 + 10^4$ Å) with THF as the eluent with a flow rate of 0.8 mL/min. These molecular weights are "nominal," based upon poly(methyl methacrylate) (PMMA) standards. Dual detectors (refractive index and fluorescence detectors) were used to detect the presence of the donor and acceptor dyes and to ensure randomly labeling of the polymer chains.[14] When secondary nucleation during the synthesis was suspected, the samples were analyzed by atomic force microscope (AFM). The analysis was made by contact mode on a freshly formed film, cast on a square quartz substrate from a dilute latex dispersion (about 5 wt% solids). The latex characteristics are summarized in *Table* 4.

## Film Formation, Annealing, and Fluorescence Measurements

Labeled latexes were used for fluorescence measurements. Some experiments involved latex dispersions cleaned by ion exchange. The films used for ET experiments were prepared as follows: first, a few drops of latex dispersion (containing a 1:1 ratio of mixed Phe- and An-labeled particles, 10 wt% solids) were spread on a small quartz plate (20 × 10 mm). The plate was then placed in a covered Petri dish in order to slow down the drying process and to allow drying to proceed at high relative humidity. Drying occurred in an air-flushed oven pre-warmed to 30°C. Under these conditions transparent films were formed over a period of seven hours. The films, on their substrates, were then annealed at a higher temperature for various periods of time. Films to be annealed for short periods of time were placed directly on a high-mass aluminum plate in an oven preheated to the annealing temperature. Films heated for more than two hours were heated under nitrogen in quartz tubes sealed with a septum. For fluorescence decay measurements, the labeled films were placed in a similar quartz tube and degassed with $N_2$.

The preparation of films to be used for the mechanical studies was slightly different. First dispersions of both the Phe- and An-labeled particles were mixed in a 1:1 ratio. Then the mixed dispersion (solids content 25 wt%) was degassed by evacuation to 10 to 15 Torr followed by re-exposure back to atmospheric pressure. This process was repeated a dozen times. Finally the dispersion was poured into an all-Teflon mold, 20 cm × 12 cm, 6.0 mm deep.

The mold was then placed into a still air environment in a pre-warmed drying oven (Baxter, vacuum drying oven model DP-32) at 39°C for a period of 48 hr. The oven door was kept closed in order to maintain high humidity in the oven. Slowing down the drying process in this way is essential for obtaining uniform films. The only venting of the oven to the outside was through the port normally used to pull a vacuum in the oven. The films obtained were free of air bubbles and presented a nice and smooth uniform surface. We prepared films with an average thickness of 0.8 mm. For each type of morphology a single large film was prepared. Then three or four sections were cut from the film and these sections were annealed for different times at 80°C. For each annealing time, a portion of the film was cooled to room temperature and the phenanthrene fluorescence decay profile was measured in order to assess the extent of polymer diffusion in the sample. From the rest of the film, we cut test samples for both dynamic mechanical analysis and tensile experiments.

Fluorescence decay measurements employed the single photon timing technique,[15] as described previously,[8,9,16] using a pulsed deuterium lamp as the excitation source.

## Dynamic Mechanical Analysis

Measurements of the polymer moduli (G', G'') were made using a Rheometrics Model RAA dynamic mechanical analyzer in the parallel plate geometry (2.5 cm diameter plates). An oscillating shear strain was applied to the sample via the lower plate, which rotates sinusoidally about a certain angle, and the resulting shear stress is measured as the torque at the upper plate. In our system the most interesting part appeared to be located at high temperature, in the "flow region" (around the G'/G'' crossover). To focus on this region for each type of latex film, we carried out a frequency/temperature sweep. This test consists of several frequency sweeps at fixed temperature. At each temperature, the frequency ω was varied from $10^{-2}$ to $10^2$ rad/s. Then, using the time-temperature superposition (TTS) principle,[17] we constructed a master curve that covers a wider range of frequencies at a characteristic temperature. In this way

we were able to observe differences in behavior induced by the different types of crosslinking morphology in our systems. In order to maintain a torque value within the operating range of the machine, it was necessary in some cases to increase the percent strain as the signal diminished with increasing temperature (and decreasing frequency). To ensure linear viscoelastic strain behavior, all samples were tested by performing a strain sweep at both the initial and the final temperature.

Even so, for some samples, some of the data collected at low torque values were at the limit of the rheometer sensitivity. This sensitivity limit accounts for the scatter in the data points at very low frequency on the master curves. The sweeps were made at five different temperatures between 100° and 280°C. The master curves were calculated for a reference temperature of 184°C. We were initially concerned about the possibility of sample decomposition at the high temperature end. We found that once a frequency sweep test was complete, a new frequency sweep on the same sample at the same or lower temperature gave the same results.

### Tensile Testing

Standard tensile test specimens were cut from the latex films using a metallic die (similar to that described in ASTM D 1707-84). The cut specimens had the following shape:

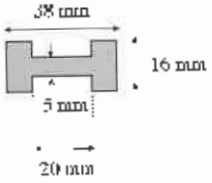


The tensile tests were carried out in a room in which the temperature and humidity were kept constant and monitored (21°C/50% RH). The test specimens were placed in the test room 24 hr prior to carrying out the tensile measurements, in order to allow the samples to equilibrate with the room temperature and humidity. The testing machine was equipped with pneumatic clamps. In this way the pressure applied on the specimen remained constant throughout the test and constant from sample to sample.

The deformation was followed by recording the crosshead displacement, employing a displacement speed of 19 mm/min. For each type of film, for each annealing time, tensile tests were repeated at least on four samples to assess the reproducibility and to calculate the standard deviations for the measurement. Unfortunately, due to some sample imperfections that led to a material shortage (failure in the film formation), we sometimes had to limit ourselves to tests on two or three samples.

## FLUORESCENCE DATA AND DATA ANALYSIS

Many experiments described are based upon Förster non-radiative energy transfer[18,19] between a donor dye D, which is selectively excited, and a second dye, the acceptor A. The attractive feature of this process is that the rate of energy transfer w(r) depends sensitively on the distance r between the donor and acceptor chromophores, $w(r) = (1/\tau_0)(R_0/r)^6$, in which $\tau_0$ is the donor fluorescence lifetime in the absence of acceptors, and $R_0$ is the characteristic distance (the Förster distance) over which ET takes place. Typical values of $R_0$ are 2 to 5 nm. Thus ET measurements represent a powerful method to measure distances, or the distribution of distances, in complex samples. In our experiments, the D and A groups are attached to the backbone of individual polymer molecules. ET experiments measure the rate or extent of processes that bring D and A groups together, or cause them to move apart. For the phenanthrene-anthracene pair employed here, $R_0 = 2.3$ nm.[8b]

In a system with uniformly distributed donors and acceptors in three dimensions, the donor fluorescence intensity decay $I_D(t)$, following a δ-pulse excitation, is described by equation (1), where P is proportional to the acceptor (quencher) concentration [Q][18,19]:

$$I_D(t') = B\exp\left[-\frac{t'}{\tau_0} - P\left(\frac{t'}{\tau_0}\right)^{1/2}\right] \quad (1)$$

$$P = \gamma\frac{4\pi^{3/2}N_A R_0^3[Q]}{3000} \quad (2)$$

In equation (2), γ is an orientation factor, and $N_A$ is Avogadro's number. B, the pre-exponential term, represents the fluorescence intensity at $t' = 0$.

The quantum efficiency of energy transfer $\Phi_{ET}$ is defined as[20]

$$\Phi_{ET} = 1 - \frac{\int_0^\infty I_D(t')dt'}{\int_0^\infty I_D^0(t')dt'} \quad (3)$$

where $I_D(t)$ and $I_D^0(t)$ are the decay functions of donor fluorescence in the presence and absence of acceptor, respectively. The integrals of the donor emission in equation (3) can be evaluated from the areas obtained experimentally under the donor decay curves (normalizing the decay curves at decay time zero),[16] giving

$$\Phi_{ET} = 1 - Area(t)/Area_D^0 \quad (4)$$

where *Area(t)* and $Area_D^0$ are the areas under the normalized decay curves of donor fluorescence in the presence and absence of acceptor, respectively. The (*t*) in *Area(t)* refers to the sample annealing time. It is important to note that the integrated area under the fluorescence decay profile has units of time (ns). The decay profile of the phenanthrene donor employed here is exponential in the absence of acceptors, and the denominator in equation (3) is equal to $\tau_0$.

We monitored the polymer diffusion process by measuring changes in the extent of energy transfer between donors and acceptors attached to the polymers originally separated in individual particles. Fluorescence decay measurements were carried out on our film samples as a means of assessing the extent of energy transfer and

polymer diffusion as a function of the thermal history. To characterize the diffusion process, we calculated the extent of mixing due to diffusion by comparison of the fluorescence decay curves. In simple systems where one examines small molecule diffusion in polymers, or the diffusion of polymers in a sample with a very narrow molecular weight distribution, this calculation can be done in a rigorous manner, so that one can calculate the center of mass diffusion coefficients of the diffusing species.[10,16b] Here, the situation is much more complex. The polymers themselves have a relatively broad distribution of chain lengths and the molecular weight of the sample increases to infinity for the crosslinked particles.

A simple measure of the fraction of mixing, $f_m(t)$, is the normalized growth in energy transfer efficiency[16]

$$f_m = f_m(t) = \frac{\Phi_{ET}(t) - \Phi_{ET}(0)}{\Phi_{ET}(\infty) - \Phi_{ET}(0)} = \frac{Area(0) - Area(t)}{Area(\infty) - Area(t)} \quad (5)$$

where $[\Phi_{ET}(t) - \Phi_{ET}(0)]$ represents the change in energy transfer efficiency between the initially prepared film and that aged for time t. In our experience, the most reliable way to obtain $\Phi_{ET}$ is from the area under the normalized fluorescence decay curve. To obtain an accurate area for each decay profile, we fit the profile to a not entirely arbitrary mathematical function:

$$I_D(t') = A_1 \exp[-t'/\tau_D - P(t'/\tau_D)^{1/2}] + A_2 \exp(-t'/\tau_D) \quad (6)$$

The physical meaning of the fitting parameters ($A_1$, $A_2$, P) in equation (6) are not important here, but one can use these parameters to calculate the area under the normalized decay profile by integrating $I_D(t')$ from time zero to infinity. The $f_m(t)$ values are obtained by comparing areas under the measured decay profiles for films without aging [*Area(0)*], aged for certain times [*Area(t)*], and aged for a sufficiently long time to approach a minimum value of area [*Area(∞)*]. Here we obtained the *Area(∞)* value using a solvent-cast film, prepared from a model latex with no crosslinking.

## RESULTS AND DISCUSSION

### Design, Preparation, and Characterization of Latex Samples

By seeded emulsion polymerization under monomer-starved conditions, we prepared a series of acrylate copolymer latex samples in which the fundamental monomer composition was BMA plus butyl acrylate (BA), with a BMA/BA ratio of about 10/1. Crosslinked particles were obtained by adding 1 mol% of EGDMA to the monomer feed. In all of these samples, the $T_g$ of the copolymer is approximately 20°C. To obtain structured latex in which the reticulation was confined to only a portion of the particle, the emulsion polymerization was carried out in three successive stages. EGDMA was added to the seed-plus-second-stage to obtain core-crosslinked particles. Alternatively, the seed and second stage of the polymerization was free of difunctional monomer, and the EGDMA was incorporated only into the third stage of the reaction.

All the experiments described involve pairs of latex prepared from a common seed latex. The seed is unlabeled and represents as much as 35% of the particle volume for two-stage polymerizations, and a significantly smaller fraction in the three-stage emulsion polymers. In each pair, one is labeled with phenanthrene (Phe) as the donor (D) chromophore, and the other is labeled with anthracene (An) as the acceptor (A) chromophore for direct non-radiative ET experiments. The phenanthrene group is introduced using 9-vinylphenanthrene as a comonomer. The anthracene group is introduced using 9-anthryl methacrylate as a comonomer. In some instances where this monomer was used, the particle size was somewhat smaller than that anticipated from the size of the seed particles and the amount of monomer added.[21]

Through ET experiments, we hoped to examine three features of the films produced from these crosslinked or partially crosslinked latex. Our first concern is the influence of uniform crosslinking on polymer diffusion in latex films. The second topic is the influence of the location of crosslinks in a core-shell latex on polymer diffusion. The third feature concerns the influence of morphology on ET in core-shell latex films. We wished to examine whether ET experiments on films prepared from selectively labeled latex can provide insights into the particle morphology.

To examine the influence of crosslinking on polymer diffusion in latex films, we synthesized two types of latex particles by two-stage emulsion polymerization. One pair of latexes consists of linear polymer; the other, of uniformly crosslinked polymer. Their particle structure is indicated in the drawings below. In this notation, $L^D$ refers to a latex consisting of linear uncrosslinked polymer, and $X^D$ refers to uniformly crosslinked particles. The superscript ($^{D,A}$) refers to the fluorescent label. With the exception of the seed, which is unlabeled, the label distribution is uniform across the particles.


$L^D$ $L^A$ $X^D$ $X^A$

In most of the latex samples described here the extent of labeling is 1 mol% in the labeled domains. In the structured latex described in the following, only the crosslinked component is labeled, the chromophore content of this domain is 1 mol%. In the latex samples composed of a linear polymer, the non-seed portion contains a lower amount of chromophore. In one pair of dispersions, the label content is 0.15 mol%. Since this is about a factor of 7 smaller than 1 mol%, we refer to the Phe- and An-labeled samples as $L^{D/7}$ and $L^{A/7}$, respectively. Another pair of uncrosslinked latex contains 0.5 mol% latex. We refer to these samples as $L^{D/2}$ and $L^{A/2}$.


$(C_{X(50)}S)^D$ $(C_{X(50)}S)^A$ $(C_{X(12)}S)^D$ $(C_{X(12)}S)^A$

To examine the issue of how the locus of crosslinking affects polymer interdiffusion in latex films, we synthesized two pairs of latex by three-stage emulsion polymerization, in which the seed and the second stage contain 1 mol% EGDMA to crosslink the core. In $C_{X(50)}S$, the core represents 50% of the particle volume, whereas in $C_{X(12)}S$, the core is much smaller. Here it comprises only 12% of the particle volume. Both the second-stage core and the third-stage shell contain a similar extent of chromophore label.

One normally uses transmission electron microscopy (TEM) to examine the morphology of latex particles designed to have a core-shell structure. To obtain contrast, one has to be able to stain one of the components selectively. The small amount of crosslinking agent we use to crosslink the second-stage polymer does not provide contrast for TEM experiments. In order to examine whether ET experiments coupled with selective labeling of the core can provide information on the morphology of the particles, we prepared particles analogous to $C_{X(12)}S$ and $C_{X(50)}S$, in which only the crosslinked core is labeled with a donor or acceptor dye.


$C^D_{X(50)}S$ $C^A_{X(50)}S$ $C^D_{X(12)}S$ $C^A_{X(12)}S$

In all syntheses, the final latex dispersion was obtained with a solids content of about 23 wt%, with particle diameters in the range of 140 nm, with a narrow size distribution. The uncrosslinked particles have a molecular weight $M_w \approx 500{,}000$ and $M_w/M_n \approx 4$. These characteristics, for each latex, are summarized in *Table* 5. In some systems, the final particle size was smaller than expected. We suspected that some secondary nucleation may have occurred during the latex synthesis. To investigate this matter further, these samples were analyzed by atomic force microscopy. The analysis indicated that the particles were monodisperse in size and showed no evidence for small particles that would be produced through secondary nucleation. These AFM images also confirmed the diameter previously measured by dynamic light scattering.[21]

## Polymer Diffusion in Films Formed from Lightly Crosslinked Latex

In films prepared from uncrosslinked latex, little or no interdiffusion occurs during film formation. Diffusion is accelerated by an increase in temperature. At 80°C, in films prepared from a 1:1 mixture of $L^{D/}$ and $L^{A/}$, interdiffusion occurs on a time scale of hours. The extent of mixing ($f_m$) approaches 1.0 after about 60 hr. The data are presented in *Figure* 1, and we see relatively little difference between films formed from the as-prepared samples that contain the salts and SDS surfactant from the emulsion polymerization, and latex cleaned with ion-exchange resin prior to film formation. For reasons to be discussed in a later section of this paper, the chromophore content for this pair of latex is lower, 0.15 mol%, than that in other systems we examined. In past experiments carried out in this laboratory,[8,9] we had little opportunity to examine the effect label content on $f_m$. According to equations (1) and (2), the rate of donor fluorescence decay $I_D(t')$ is sensitive to the local concentration of acceptors around each excited donor. As diffusion proceeds, one expects that the efficiency of ET ($\Phi_{ET}$, equation (3)), including the limiting quantum yield, will be smaller in this system than in systems with a higher chromophore content. In *Figure* 1b we see that the value of $\Phi_{ET}$ in the freshly prepared film is close to zero, but after a few minutes of annealing at 80°C, it increases to less than 0.1. The subsequent growth in ET is slow, and after about 40 hr, $\Phi_{ET}$ approaches its limiting value of 0.35. As expected, $\Phi_{ET}$ reaches its limiting value as $f_m$ approaches 1. Full mixing corresponds to polymer diffusion over a distance comparable to a particle radius.

To study interdiffusion in films prepared from lightly crosslinked latex, we examine films prepared from a sample of ($X^D$ and $X^A$) (open circles in *Figures* 2 and 3) as well as from a sample of the second-stage polymer used to synthesize core-crosslinked particles. These latex particles ($X'^D$ and $X'^A$) have a diameter of 65 nm and contain 1 mol% chromophore. Here the early stages of annealing exhibit some features in common with those in *Figure* 1: a rapid growth in $\Phi_{ET}$ and in $f_m$ over the first hour at 80°C (*Figure* 2). Pronounced differences appear at longer annealing times. The most striking feature of the data in *Figures* 2 and 3 is that the extent of mixing appears to level off after about two hours. For ($X'^D$ and $X'^A$), the

**Table 5—Recipes for the Preparation of the Unlabeled Third-stage (Shell)-Crosslinked Particles and the Labeled Fully Crosslinked Particles**

| Materials | SX | $X^D$ | $X^A$ |
|---|---|---|---|
| **Step 2: Feed** | | | |
| Seed[c] | 10.87 ($S_X$1) | 21.8 ($S_X$1) | 21.7 ($S_X$1) |
| BMA | 15.482 | 6.37 | 6.373 |
| BA | 1.523 | 0.634 | 0.626 |
| EGDMA | — | 0.107 | 0.110 |
| V-Phe | | 0.1 | — |
| 9-AnMA | — | — | 0.131 |
| Water | 42.5 | 18 | 17.5 |
| KPS | 0.066 | 0.026 | 0.027 |
| SDS | 0.08 | 0.033 | 0.034 |
| **Step 3: Feed** | | | |
| Seeds[b] | 40.69 | 15.8 | 9 |
| BMA | 9.381 | 28.475 | 17.4 |
| BA | 0.964 | 2.793 | 1.711 |
| EGDMA | 0.149 | 0.447 | 0.281 |
| V-Phe | — | 0.453 | — |
| 9 AnMA | — | — | 0.355 |
| Water | 20 | 62.5 | 38.3 |
| KPS | 0.02 | 0.064 | 0.039 |
| SDS | 0.2 | 0.623 | 0.384 |

(a) Weight of dispersion of the seed particles. The seed dispersion employed (here 5-1) is indicated in parentheses. All amounts are in grams.
(b) Refers to the weight of latex dispersion from the previous step.

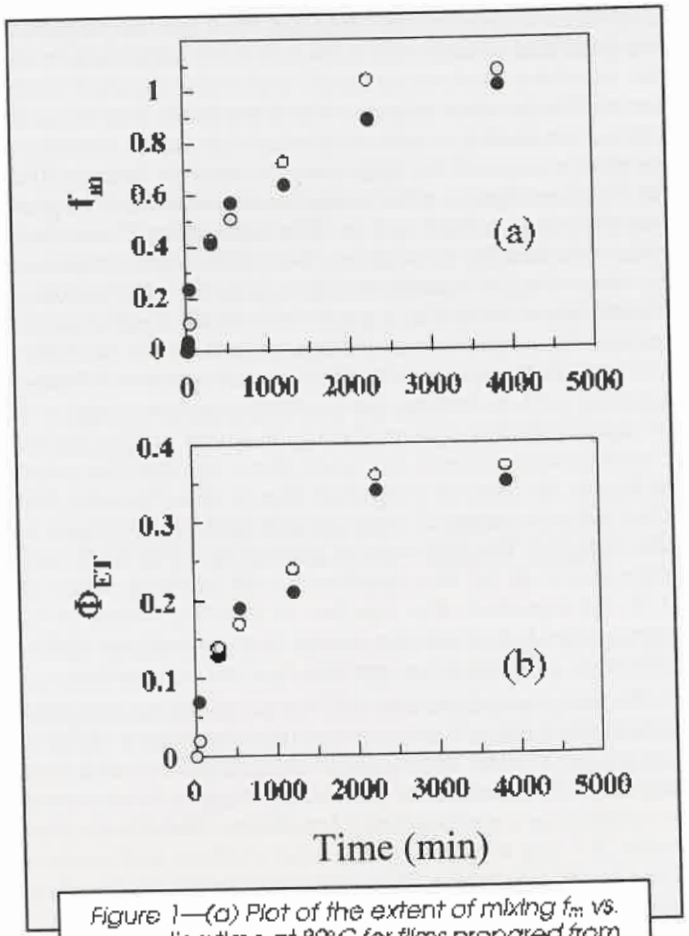


*Figure 1—(a) Plot of the extent of mixing $f_m$ vs. annealing time at 80°C for films prepared from a 1:1 mixture of Phe- and An- labeled uncrosslinked latex particles ($L^{D/7} + L^{A/7}$), particles. (b) Plot of the quantum efficiency of energy transfor $\Phi_{ET}$ vs. annealing time for this film. Open points refer to films formed from the raw latex. Closed points refer to a film obtained from latex dispersions treated with an ion-exchange resin to remove salts and ionic surfactant. Cleaning the latex in this way has a negligible effect on the rate of polymer diffusion.*

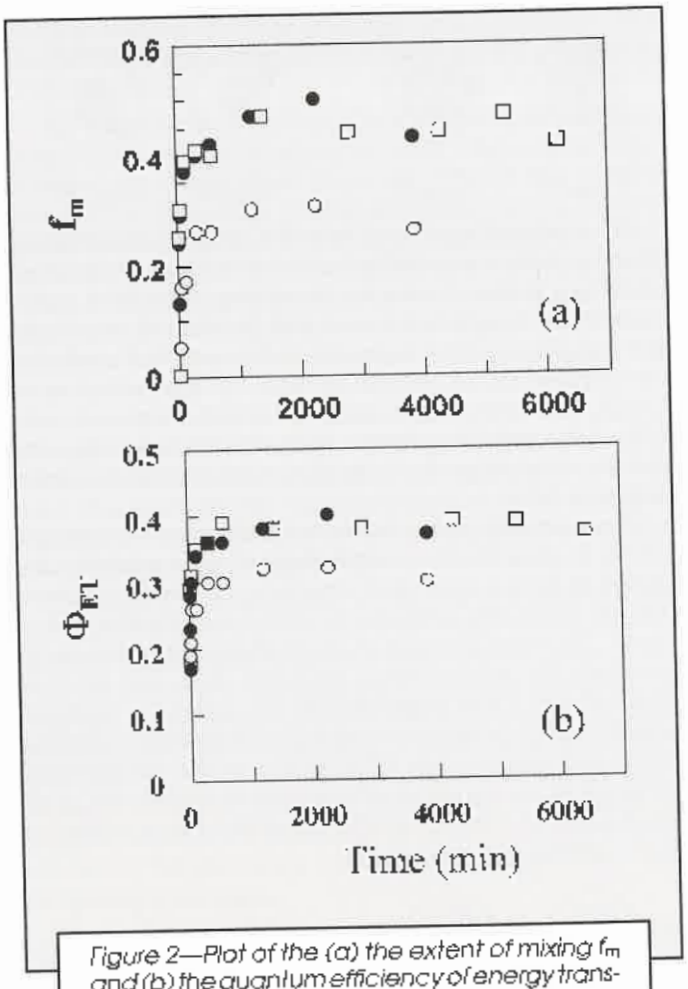


*Figure 2—Plot of the (a) the extent of mixing $f_m$ and (b) the quantum efficiency of energy transfer as a function of annealing time at 80°C, for films prepared from a 1:1 mixture of Phe- and An- labeled crosslinked particles with a diameter of 65 nm. ($X'^D + X'^A$), and for similar particles ($X^D + X^A$) with a diameter of 145 nm (open circles). Open points refer to films formed from the raw latex; Closed points refer to film obtained from latex dispersions treated with an ion-exchange resin to remove salts and ionic surfactant.*

limiting value of $f_m$ is about 0.45 and the limiting value of $\Phi_{ET} = 0.45$. For ($X^D$ and $X^A$), the limiting $f_m$ value is less than 0.3. These results provide clear evidence that crosslinking limits the extent of interdiffusion. Since the gel content of the latex particles is high (ca. 80%), mixing cannot be due only to translational diffusion of entire polymer molecules. A significant portion of the growth in ET is due to the diffusion of long ends dangling from the network in one cell, penetrating into the network of the neighboring cell. One imagines that the extent of this interdiffusion will be a function of the crosslink density. This is an important topic to investigate in future experiments.

In *Figure* 3, one sees another interesting feature of the data. In the newly formed film, prior to annealing, $\Phi_{ET} = 0.18$. Since little or no polymer diffusion occurs under these conditions, we attribute this result to ET across the interparticle boundaries between adjacent Phe- and An-labeled cells.[2] Very little ET was observed for the nascent film in *Figure* 1. There are two differences between the samples. First, the particles used to prepare the films described in *Figures* 2 and 3 are significantly smaller, 65 nm versus 140 nm for the uncrosslinked latex. These films have a much higher surface-to-volume ratio. In addition, these particles have a higher chromophore content. The Phe-groups adjacent to the cell boundary sense much higher local concentration of An-groups on the other side of the interface.

## Polymer Diffusion in Films Formed from Core-Crosslinked Latex

CORE-LABELED; SHELL UNLABELED: We first considered the example of a film prepared from core-crosslinked latex, in which the crosslinked core is small (12% of the particle volume), and only the core is labeled ($C^D_{x(12)}S + C^A_{x(12)}S$). In designing this experiment, we thought that we would observe no energy transfer in the newly formed film if the crosslinked cores were completely encapsu-

lated by the uncrosslinked (and unlabeled) shell. Under these circumstances, individual cores, labeled to the extent of 1 mol% with either Phe- or An- would be isolated from one another. As seen in *Figure* 4, $\Phi_{ET}$ is zero in the newly formed film and remains zero even as the film is annealed for many hours at 80°C.

The core of this latex is labeled with 1 mol% chromophore. In the event that there was uniform mixing of the core polymer with the uncrosslinked shell, the chromophore would be diluted by a factor of about 8. If this were to occur, the chromophore concentration would be similar to that of the uncrosslinked latex examined in *Figure* 1. The data in *Figure* 1 indicates that even with this low concentration of acceptors, a significant and measurable amount of ET would occur.

The second example we consider is a film prepared from core-crosslinked latex, in which the crosslinked core is substantial (50% of the particle volume), and only the core is labeled ($C^{D}_{X(50)}S$ + $C^{A}_{X(50)}S$). Here we find that there is no energy transfer in the newly formed film. $\Phi_{ET}$ remains zero for films annealed for up to an hour at 80°C, and then one observes the onset of energy transfer. *Figure* 5 provides an interesting comparison of the behavior of films formed from the core-crosslinked latex and from uncrosslinked particles. The crosslinked core contains 1 mol% chromophore. Since these groups would be diluted by a factor of two if uniform mixing between the core and shell took place, we chose to make the comparison with an uncrosslinked latex in which the extent of labeling is 0.5 mol%. Both pairs of particles have diameters of ca. 140 nm. One sees in *Figure* 5 that $\Phi_{ET}$ in the nascent uncrosslinked latex film is close to zero. Polymer diffusion occurs on heating, and $\Phi_{ET}$ = 0.12 after annealing the film at 80°C for approximately 20 min. Further annealing leads to an increase in ET (*Figures* 5 and 6), with $f_m$ approaching 1.0 and $\Phi_{ET}$ approaching a limiting value of 0.45. In contrast, the film containing core-crosslinked polymer reaches a limiting value of $\Phi_{ET}$ = 0.12. The limiting $f_m$ value, calculated using the data from the

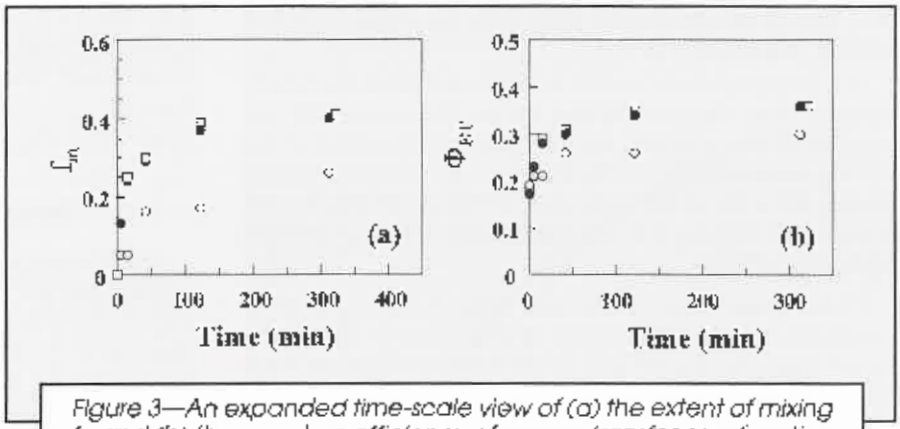


*Figure 3—An expanded time-scale view of (a) the extent of mixing $f_m$ and (b) the quantum efficiency of energy transfer as a function of annealing time at 80°C, for films prepared from the 1:1 mixture of Phe- and An-labeled crosslinked particles shown in Figure 2. The data here show the changes that occur at short annealing times.*

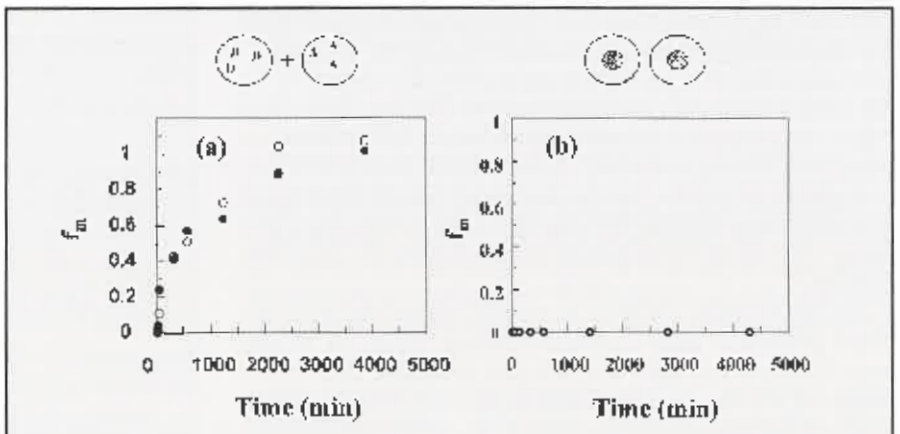


*Figure 4—Plot of the extent of mixing $f_m$ as a function of annealing time at 80°C, for films prepared from the 1:1 mixture of Phe- and An-labeled core-crosslinked (12%) latex in which only the core is labeled ($C^{D}_{X(12)}S$ + $C^{A}_{X(12)}S$). For comparison, we also plot the data for films from a 1:1 mixture of Phe- and An- labeled uncrosslinked latex ($L^{D/7}$ + $L^{A/7}$).*

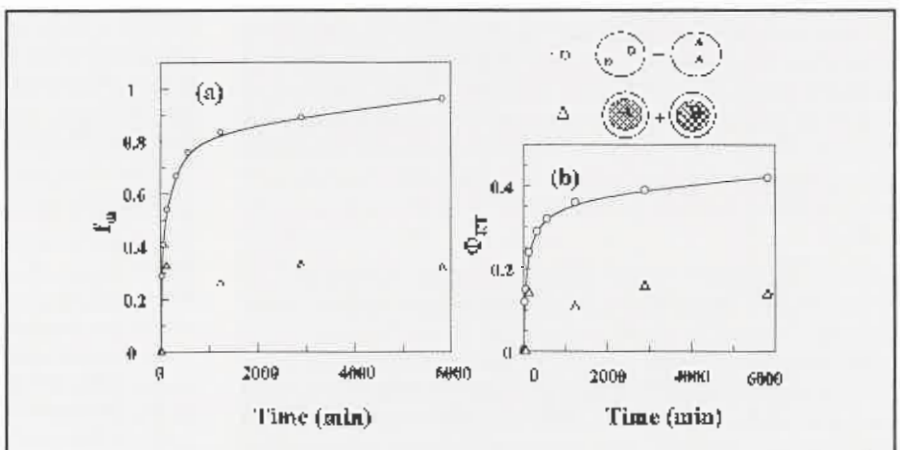


*Figure 5—Plot of (a) the extent of mixing $f_m$ and (b) the quantum efficiency of energy transfer as a function of annealing time at 80°C, for films prepared from a 1:1 mixture of Phe- and An-labeled core-crosslinked (50%) latex in which only the core is labeled ($C^{D}_{X(50)}S$ + $C^{A}_{X(50)}S$). For comparison, we also plot the data for films from a 1:1 mixture of Phe- and An- labeled uncrosslinked latex ($L^{D/2}$ + $L^{A/2}$).*

fully mixed uncrosslinked latex film as a measure of full mixing (equation (5)), is 0.3.

We interpret these results to indicate that in the newly formed film, the crosslinked cores are essentially isolated from one another. As the films are annealed, some mixing occurs. Some of this mixing is due to the approximately 20 wt% of the core that is not crosslinked, and some of the mixing may be due to coagulation of cores in adjacent particles.

Core-crosslinked; Core and Shell Labeled: Experiments to examine the extent of diffusion in films prepared from the $(CxS)^D$ and $(CxS)^A$ series of latexes were carried out differently than those described earlier. These latexes were designed to allow us to compare the growth in tensile properties of the films with the extent of interdiffusion. Fluorescence decay measurements were carried out on the same samples used for tensile testing. As a consequence, much thicker films (0.5 to 0.8 mm) were prepared, and these required much longer drying (days) at a slightly higher temperature (39°C). Some interdiffusion occurred during film preparation. To calculate $f_m$, we need a value of *Area(0)* (equation (5)). To obtain this value, we prepared thinner latex films at 30°C similar to those described previously. These 50 μm thick films dry in a matter of hours, conditions under which little or no interdiffusion occurs. We use the area under the $I_D(t')$ decay curves of these newly formed films to calculate *Area(0)*.

At early times, plots of $f_m$ versus annealing time for films prepared from core-crosslinked latex, in which both the core and shell are labeled, resemble the curves obtained for the uncrosslinked latex with 1 mol% label. There is an immediate increase in $f_m$, which reaches 0.3 ($\Phi_{ET}$ = 0.3) in about 20 min at 80°C. At later times, the behavior is different: the systems reach limiting values of $f_m$ = 0.5 ($\Phi_{ET}$ = 0.4) for $[(C_{x(50)}S)^A + (C_{x(50)}S)^D]$ and $f_m$ = 0.65 ($\Phi_{ET}$ = 0.5) for $[(C_{x(12)}S)^A + (C_{x(12)}S)^D]$. The corresponding limiting value for thick films of the fully crosslinked latex is $f_m$ = 0.4. Unfortunately, we do not have data to report on interdiffusion in films prepared from third-stage crosslinked latex.

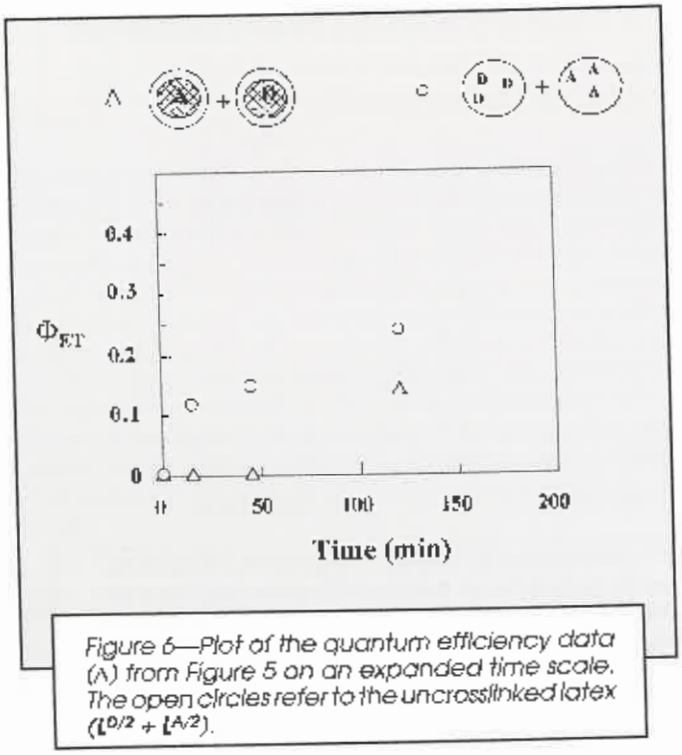


*Figure 6—Plot of the quantum efficiency data (Δ) from Figure 5 on an expanded time scale. The open circles refer to the uncrosslinked latex ($L^{D/2} + L^{A/2}$).*

## Dynamic Mechanical Properties

Oscillatory shear measurements of G′ and G″ were carried out for film samples in the parallel plate geometry. Individual experiments involved variation of frequency at constant temperature. The working temperature range for these experiments was 100° to 280°C, and each measurement lasted about 2.5 hr. Under these conditions, extensive polymer diffusion takes place. Individual measurements gave results that were independent of thermal history for samples annealed at 80°C, the conditions of the ET experiments reported previously.

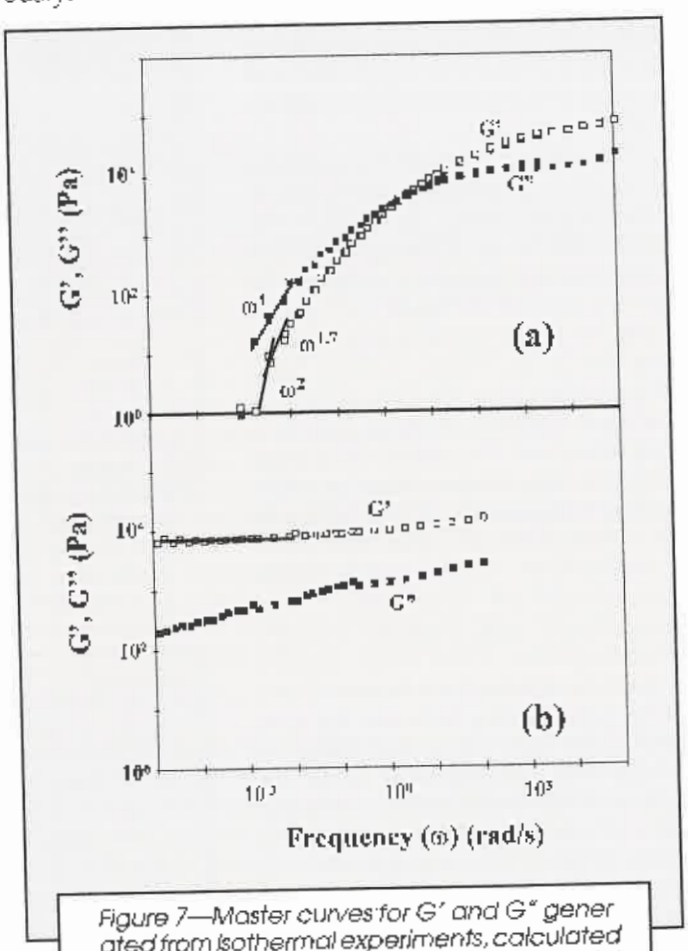


*Figure 7—Master curves for G′ and G″ generated from isothermal experiments, calculated for a reference temperature of 184°C. We plot as G′ and G″ vs. frequency (rad/s) for films prepared from (a) the uncrosslinked latex particles ($L^{D/1} + L^{A/1}$), and (b) the fully crosslinked latex particles ($X^D + X^A$). In these and other examples reported here (with the exception of the third-stage crosslinked latex), dynamic mechanical measurements and tensile were carried out on a 1:1 mixture of Phe- and An-labeled latex in which both the second- and third-stage polymer have a similar level (1 mol%) of label.*

For each of the samples examined, master curves were calculated from the set of frequency/temperature experiments. The shapes of these curves depend upon the presence and location of crosslinking in the sample. We first consider the two extreme situations: latex films formed from uncrosslinked and fully crosslinked particles. The master curves for these two systems are presented in *Figures* 7a and 7b, respectively.

For films formed from the uncrosslinked particles, the behavior observed for G′ and G″ is typical of that observed for uncrosslinked polymer with a broad molecular weight distribution. At low frequency, the mechanical properties are governed by viscous flow. One expects a power law dependence of G′ and G″ in the stress-strain behavior, with $G' \sim \omega^2$ and $G'' \sim \omega^1$ at low frequency.[23] In our experiments on the uncrosslinked latex films, G″ exhibits an $\omega^1$ dependence in the low frequency range, whereas over the range of frequencies that were accessible, G′ varies as $\omega^{1.7}$. For G′ measurements, we were limited by the sensitivity of the transducer and were unable to obtain data at frequencies which exhibit an $\omega^2$ dependence. A line showing the $\omega^2$ slope is shown in *Figure* 7a as a dotted line.

In the case of films formed from fully crosslinked particles (*Figure* 7b), the behavior is quite different. G′ reaches a constant value (ca. $7.7 \times 10^5$ Pa) in the limit of low frequency, and G″ is much smaller than G′. This polymer exhibits rubber-like elasticity, and G′ and G″ behave as predicted by the theory of rubber elasticity.[24]

To lay the basis for understanding the dynamic mechanical behavior of the films prepared from partially crosslinked latex, we considered the consequences of introducing crosslinks into an uncrosslinked matrix. We pictured these effects in the drawing in *Figure* 8, in which we generalize the data in *Figure* 7a to represent the general case of an entangled but uncrosslinked polymer film. As one introduces crosslinks, the film becomes more elastic. G′ increases, particularly in the low frequency regime, since the crosslinks suppress polymer flow. G″ also increases at low frequency. At higher frequencies, one expects an increase in the plateau modulus $G_N^0$. In terms of the simple theory of rubber elasticity, $G_N^0$ is proportional to the number of mechanically active chains, which in turn depends upon the sum of the number of chemical crosslinks in the system plus the number of physical crosslinks due to entanglements.

The linear dynamic mechanical properties of the films formed from the structured latex is intermediate between that of the uncrosslinked and fully crosslinked latex films. The data are shown in *Figure* 9. In *Figure* 9a the films formed from the core-crosslinked particles $C_{X(12)}S$, in which the crosslinked core represents only 12% of the particle volume, resemble films of uncrosslinked latex. The G′/G″ crossover is shifted to somewhat higher frequency and higher modulus. One still observes viscous flow at low frequency, but here G′ decreases as $\omega^{0.9}$ and G″ decreases as $\omega^{0.7}$. Because only a small fraction of the total polymer volume is crosslinked, one observes mainly the response of the uncrosslinked matrix.

There is a significantly greater effect in films of $C_{X(50)}S$, in which the crosslinked core comprises 50% of the particle volume (*Figure* 9b). The film gains resistance to deformation, particularly at low frequencies. The G′ and G″ curves lie virtually on top of one another and both become proportional to $\omega^{0.52}$. Polymers near the gel point commonly exhibit such a power-law dependence in this frequency range.[25,26]

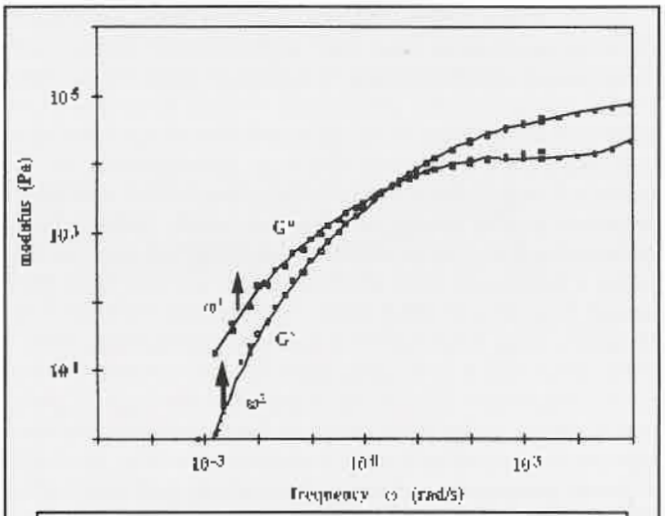


*Figure 8—A representative plot of G′ and G″ vs. frequency for an uncrosslinked entangled polymer of broad molecular weight distribution with arrows indicating the change anticipated in G′ and G″ at low frequency as crosslinks are introduced into the system.*

In contrast to the films prepared from the core-crosslinked latex, the films prepared from the third-stage (shell)-crosslinked latex ($CS_{X(50)}$, *Figure* 9c) are more rigid. There is still a tendency for viscous flow at low frequency. There is no clear expression of a plateau modulus at high frequency, and we no longer observe a G′/G″ crossover. Here, in the low frequency limit, we observe an increase of G′ with $\omega^{0.35}$ and G″ with $\omega^{0.53}$. Comparing the data in *Figures* 9b and 9c, we note that the frequency dependence of G″ does not seem to be affected by the difference of morphology, which would suggest that G″ is primarily sensitive to the global extent of crosslinking in the film. The G′ data are very different, particularly at low frequency. The importance of this result is that it demonstrates that in latex films formed from partially crosslinked particles, the elastic modulus depends not only on the extent of crosslinking but the particle morphology as well.

The sensitivity of G′ and G″ to the morphology of the latex used to form a film is not unexpected. Our observations remind us of the classic work of Lambla et al.,[27] who prepared a series of latexes from a common mixture of acrylate monomers (methyl methacrylate + butyl acrylate). Depending on the nature of the monomer feed into the reaction (staged feed, starved feed, power feed), particles of different (but uncharacterized) morphology were formed. Films formed from these various particles had very different dynamic mechanical properties. These authors were primarily interested in the temperature dependence of G′, G″, and tan δ, since the position of the glass transition was an important signature of the film morphology for these copolymer films.

There is an interesting comparison between two of their experiments and our experiments with core-crosslinked and third-stage crosslinked particles. Lambla et al.[27] compared the properties of films prepared from latex resulting from two different two-stage emulsion polymerizations. In one, BA was polymerized in the presence of a PMMA seed; in the other MMA was polymerized in the presence of a BA seed. Although no morphological characterization is reported, one anticipates a hard-core/soft shell structure for the latex produced from the PMMA seed. The second reaction with the PBA seed might give the inverse structure, with a hard shell and a soft core. Both latexes contain 50% of each component. The authors find that the high $T_g$ polymer formed in the final stage of the emulsion polymerization is more effective at increasing the film modulus at room temperature than if the high $T_g$ polymer forms the core. We find that introducing crosslinks in the final stage of the emulsion polymerization has a much more important effect on G′ at low frequency than the same volume of crosslinked polymer present in the core. The dynamic mechanical data for this system are in fact quite unusual in that G′ remains above G″ at all frequencies, but the curve exhibits a kink which virtually touches the G″ curve at a modulus of $10^5$ Pa and a frequency near $10^{-1}$ rad/s. The system behaves like an uncrosslinked but entangled polymer above the kink, with a crossover to a crosslink-dominated behavior at lower frequencies.


While we do not have evidence about the morphology of the particles formed when the crosslinked polymer is added in the final stage of the polymerization, we doubt that a separate crosslinked shell phase is formed. For our system in which the final stage polymer is chemically almost identical to the polymer already present, it

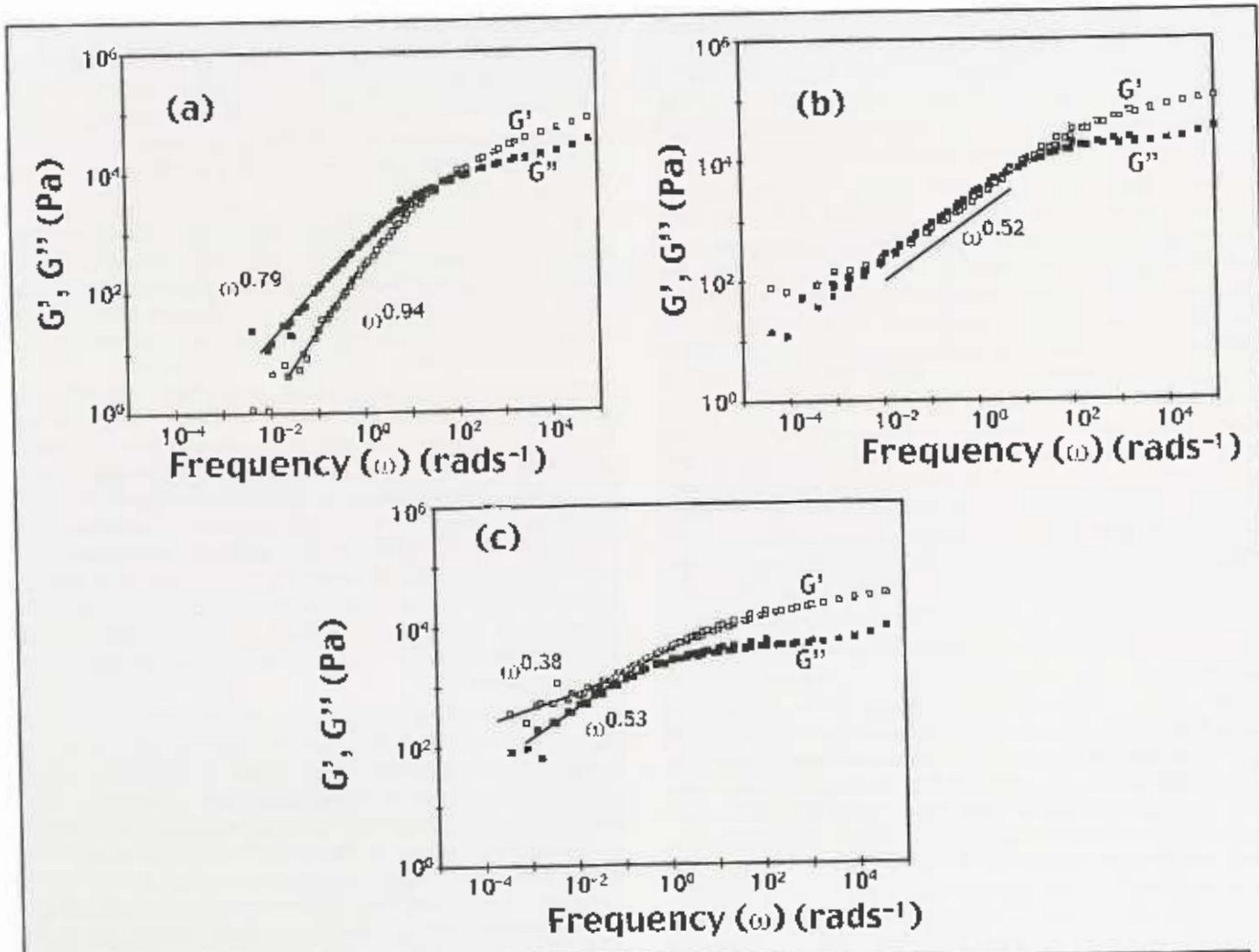


*Figure 9—Master curves for G′ and G″ generated from isothermal experiments, calculated for a reference temperature of 184°C. We plot as G′ and G″ vs. frequency (rad/s) for films prepared from (a) the core-crosslinked (12%) latex particles, (b) the core-crosslinked (50%) latex particles, and (c) the third-stage-crosslinked (50%) latex particles.*

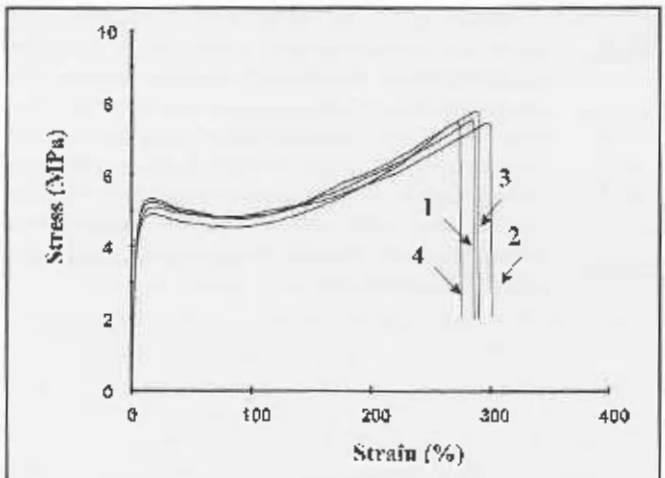


*Figure 10—Stress-strain plots for four film samples of the core-crosslinked (50%) latex annealed for two hours at 80°C, cooled to room temperature, and equilibrated 24 hr at 50% RH before tensile tests were carried out. The sample-to-sample differences observed here are typical (rather than best-case) of the tensile experiments on the various latex films reported.*

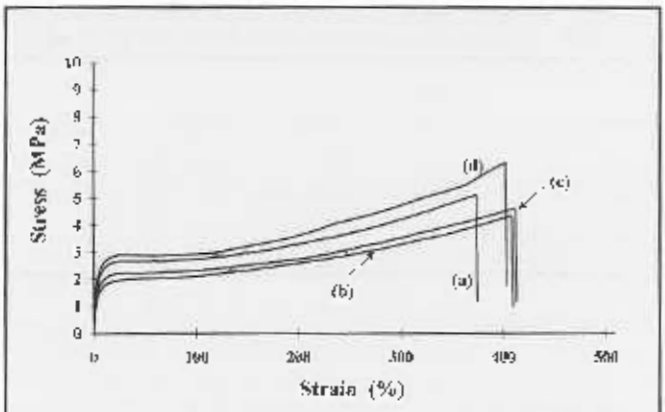


*Figure 11—Stress-strain plots for four samples of latex films prepared from the uncrosslinked latex ($L^{0/1} + L^{A/1}$), but subjected to different thermal histories: (a) not annealed ($f_m = 0.1$). Annealed at 80°C for (b) 2.3 hr ($f_m = 0.3$); (c) 12 hr ($f_m = 0.4$); (d) 105.2 hr ($f_m = 0.6$). In these and other examples reported, tensile tests were carried out on a 1:1 mixture of Phe- and An-labeled latex in which both the second- and third-stage polymer have a similar level (1 mol %) of label.*

is likely that the monomer sorbs into the seeds, and that polymerization takes place within the existing particles. Even in the case of redox initiation and polymerization at room temperature, the polymerization takes place above the $T_g$ of the seed phase. If polymerization occurs uniformly in the particle, a semi-interpenetrating network (semi-IPN) will form. If the crosslinked polymer phase separates as it forms, dispersed droplets of the crosslinked phase will form in the particle interior. We depict these two possibilities in the drawings. We would like to emphasize that there should be a significant difference in properties between the semi-IPN morphology and the case of a "core-crosslinked" structure with the core strongly swollen by the third-stage uncrosslinked polymer. When the crosslinked core is formed first, swelling of the core by the linear polymer is resisted by the deformation entropy of the crosslinked network. In the semi-IPN structure, the crosslinked network is formed in the presence of the linear polymer. This promotes a looser structure, with linear polymer entangled into the chemically crosslinked network.

The rheological behavior observed in *Figure* 9c is reminiscent of that reported by Cavaillé et al.[28] for films prepared from a blend of hard and soft latex particles. This kind of stress-strain behavior was attributed to a percolation of the hard polystyrene particles in the soft poly(butyl acrylate) matrix. The similarity in stress-strain behavior may favor a morphology for our third-stage crosslinked latex of a dispersed crosslinked phase that formed a percolation network upon annealing.

We dwell on these arguments because we find the mechanical properties of this system truly fascinating. From a technological point of view, the results we describe suggest that one may obtain more effective control over the mechanical behavior of a film-forming latex system using by varying the extent of crosslinking and confining the crosslinking agent to the final stage of the emulsion polymerization. This is a topic well worthy of a more detailed investigation.

### Tensile Properties of the Films

Almost all of the films used in the tensile experiments were prepared from a 1:1 mixture of Phe- and An-labeled latex. With these samples, we could measure the corresponding extent of interdiffusion that took place. Tensile measurements were carried out on thicker films (0.5 to 0.8 mm) than those used for many of the ET experiments described previously. In order to obtain smooth and defect-free films, the dispersions were dried slowly (over three days) at 39°C. After dog bone samples were cut from the film, these samples were aged for 24 hr at 20°C and 50% RH. Under this combination of circumstances, a small but significant extent of polymer diffusion across the intercellular boundaries takes place, and we find that $f_m > 0$ in the unannealed films. We measured the evolution of tensile strength and the extent of interdiffusion that occurred as the films were subsequently annealed at 80°C.

Tensile measurements require great care since defects in the sample can lead to premature rupture. The films formed from the fully crosslinked latex were the most delicate. For each set of five samples examined, one or two had a significantly lower strain-at-break than the others. Here we discarded the data from these samples and averaged the results of the remaining three or four samples. We should emphasize, however, that none of the samples were brittle. They formed tough elastomeric films. Even the worst case sample, a premature break in a fully crosslinked film, exhibited a strain-at-break of

**Table 6—Young's Modulus Values (E, MPa) Determined from Tensile Measurements on Latex Films Prepared from Structured and Unstructured Latex**

| Annealing | Latex L | $C_{x(12)}S$ | $C_{x(50)}S$ | $CS_x$ | X |
|---|---|---|---|---|---|
| None | 76 ± 7[a] | 85 ± 16 | 130 ± 10 | 100 ± 15 | 220 ± 20 |
| 100+ hr[b] at 80°C | 64 ± 7 | 200 ± 15 | 170 ± 15 | 130 ± 20 | 190 ± 15 |

(a) One standard deviation.
(b) 100.2 hr for sample L, 119.3 hr for the other samples.

over 150%. A more typical example is shown in *Figure* 10, where we present stress-strain plots for four samples of a film annealed for 2 hr at 80°C, prepared from a core-crosslinked latex (50% core volume). For each curve, we determine the stress-at-break ($\sigma_b$, the tensile strength), the strain-at-break ($\varepsilon_b$), the stress at the yield point ($\sigma_y$), and the slope of the stress-strain plot at low deformation (E, Young's modulus). We also calculate the toughness $W_b$, the area under the stress-strain curve. Typical standard deviation values are found to be around 8%, except in the case of the Young's modulus where the standard deviation values are found to be around 15%.

In *Figures* 10-12, we plot the data using as the y-axis [(measured force)/(initial cross-section area) ≡ $F/A_o$]. Since the films undergo elongation, the cross-section area decreases with increasing strain. For elongation by a factor of $\lambda$, the width and thickness each decrease by a factor of $\lambda^{-1/2}$. Thus, $A_\lambda = A_o\lambda$. The disadvantage of plotting $F_\lambda/A_o$ versus $\lambda$ is that the yield point is difficult to discern in the plot. Since we are more interested in comparing relative values of the yield stress and tensile strength, and these events occur at similar values of $\lambda$, we prefer to report uncorrected "engineering" values of $\sigma_y$ and $\sigma_b$, and "apparent" values of $W_b$.

EFFECTS OF ANNEALING: We first considered "engineering" values of $\sigma_y$ and $\sigma_b$, and "apparent" values of $W_b$, and the influence of annealing on the evolution of film properties. In *Figure* 11 we present a stress-strain curve for each of several annealing times for films prepared from uncrosslinked latex. The curve labeled (a) is the unannealed film. For this film, $f_m = 0.1$, implying that some interdiffusion occurred during sample preparation. The stress-strain curve is typical of an elastomer, exhibiting a strain-at-break of 375%, a tensile strength of 5 MPa, and a toughness of 12.6 MPa. When the films are heated at 80°C, polymer diffusion occurs. For curve (b) (2.3 hr), $f_m = 0.3$; for curve (c) (12 hr), $f_m = 0.4$; for curve

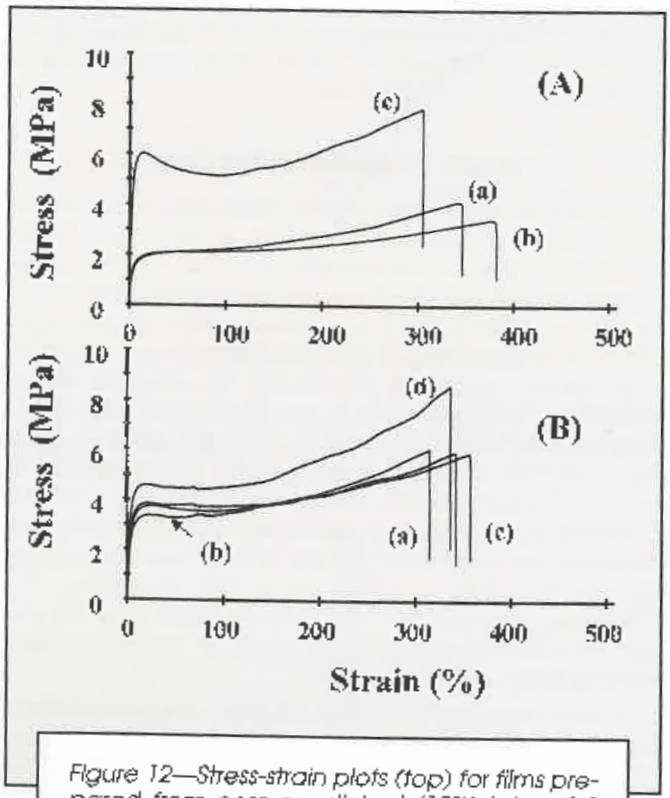


*Figure 12—Stress-strain plots (top) for films prepared from core-crosslinked (12%) latex (1:1 mixture of $(C_{x(12)}S)^D$ and $(C_{x(12)}S)^A$) for different thermal histories: (a) not annealed ($f_m$ = 0.25). Annealed at 80°C for (b) 20 min ($f_m$ = 0.3); (c) 119.3 hr ($f_m$ = 0.65). Bottom: for films prepared from third-stage-crosslinked (50%) latex for different thermal histories: (a) not annealed. Annealed at 80°C for (b) 2 hr; (c) 21 hr; (d) 119.3 hr.*

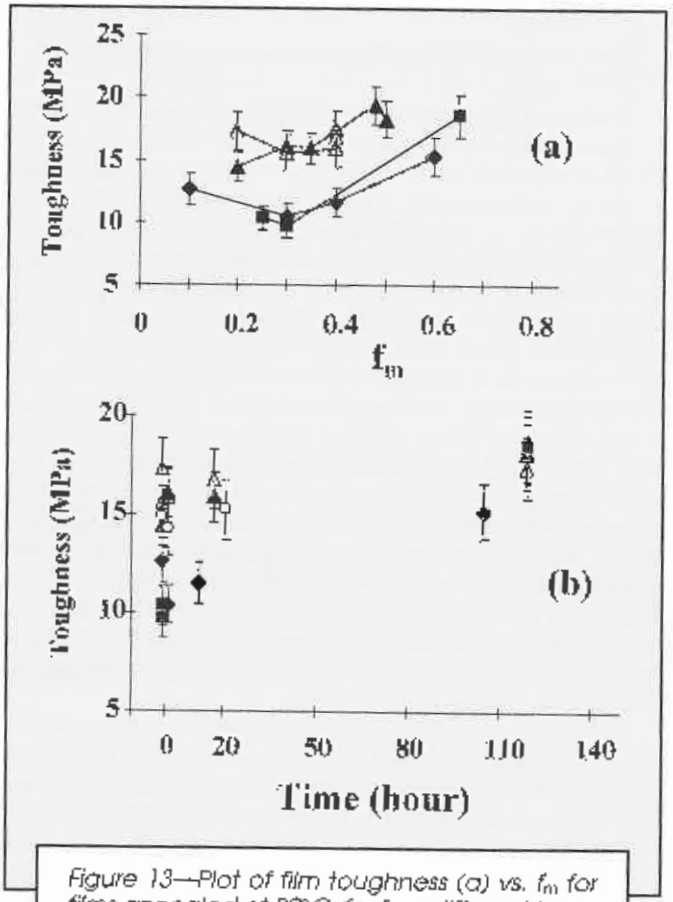


*Figure 13—Plot of film toughness (a) vs. $f_m$ for films annealed at 80°C, for four different types of latex films: (◆) uncrosslinked latex; (■) core-crosslinked (12%) latex; (▲) core-crosslinked (50%) latex; and (△) fully crosslinked latex. In (b) we plot the same data vs. annealing time and include data for films of the third-stage-crosslinked latex (○). Error bars represent one standard deviation.*

(d) (105 hr), $f_m = 0.6$. Upon annealing, the stress-at-break appears to decrease slightly before increasing. These changes are small and may not be significant. The strain-at-break exhibits a small but significant increase, but the toughness does not change very much. Most of the strength is developed as the films are formed.

This general conclusion applies to all the latex films we examined: tough elastic films form, even without annealing. Upon annealing, only relatively small changes in tensile strength and toughness occur. The most substantial changes occurred for the core-crosslinked latex (core + shell labeled) where the core represents 12% of the particle volume. The data are shown in *Figure* 12a. Although only one trace is shown for each annealing time, the different samples at each time were in excellent agreement with one another. The initially formed film ($f_m = 0.2$) had a large elongation-to-break but a relatively weak tensile strength (ca. 3 MPa). Small changes occurred following annealing at 80°C for 20 min ($f_m = 0.3$), but after extensive annealing (119 hr, $f_m = 0.65$), the films exhibited a large increase in yield stress, tensile strength, but a decrease in strain-at-break. The toughness increased from about 10 MPa (curves (a) and (b)) to 18 MPa (curve (c)).

For the third-stage crosslinked sample, where we do not have ET data, we present the evolution of the tensile properties as a function of annealing time. We see many of the features exhibited in the core-crosslinked (12%) samples. The initially formed film exhibits substantial toughness, with a yield stress of ca. 4 MPa. At the early stages of annealing (2 hr), the toughness of the film remains rather constant at 14 MPa. When annealed for 20 hr, the film still presents similar characteristics. For much longer annealing (119 hr) there is a significant increase in the yield stress and the stress-at-break. In spite of a small decrease in the strain-at-break, the toughness of the film has increased to 18 MPa.

**Effects of Latex Morphology:** From the slopes of the stress-strain curves at small deformation, we calculated values of Young's Modulus E. The presence of crosslinks in the latex has a substantial effect on the magnitude of E, which range from 76 Pa for the newly formed films of the uncrosslinked latex to 220 Pa for those of the uniformly crosslinked polymer. For unannealed films prepared from the structured latex, the E values increase with crosslink content (*Table* 6). One sees, however, that the modulus of the third-stage crosslinked latex films is lower than that of the core-crosslinked $C_{x(50)}S$ latex films, even though the crosslink content is identical. Annealing has no significant effect on the E values of the uniform latex, but interesting effects on films formed from the structured latex. For

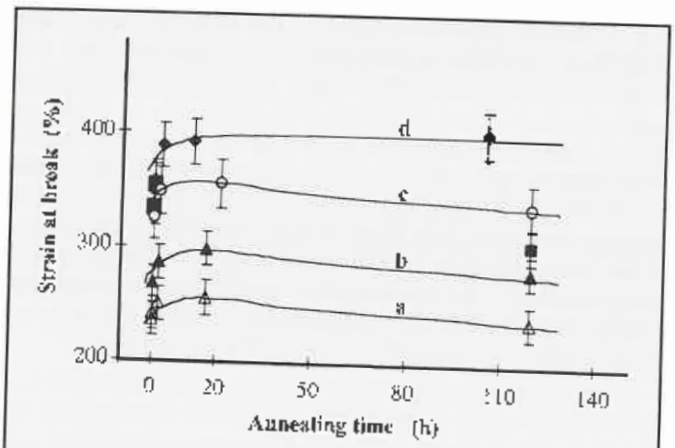


*Figure 14—Plot of strain-at-break vs. annealing time at 80°C for different types of latex films: (◆) uncrosslinked latex; (■) core crosslinked (12%) latex; (▲) core-crosslinked (50%) latex; and (Δ) fully crosslinked latex; third-stage crosslinked latex (O).*

both $C_{x(50)}S$ and $CS_x$, the modulus increases, but the E value for the core-crosslinked latex film is still larger. Some of the differences here border on experimental error. The most profound effect is on films prepared from the $C_{x(12)}S$ latex. The unannealed film shows almost no reinforcement from the presence of the small crosslinked core. Upon annealing, the modulus doubles, to be comparable to that of latex films with a 50% crosslink content.

In *Figure* 13, we show two different ways of presenting the data on the evolution of film toughness for films prepared from particles with different morphologies. In *Figure* 13a, we plot toughness versus $f_m$ for four different types of latex. For the uncrosslinked and core-crosslinked (12%) latex films, the initial toughness is relatively low

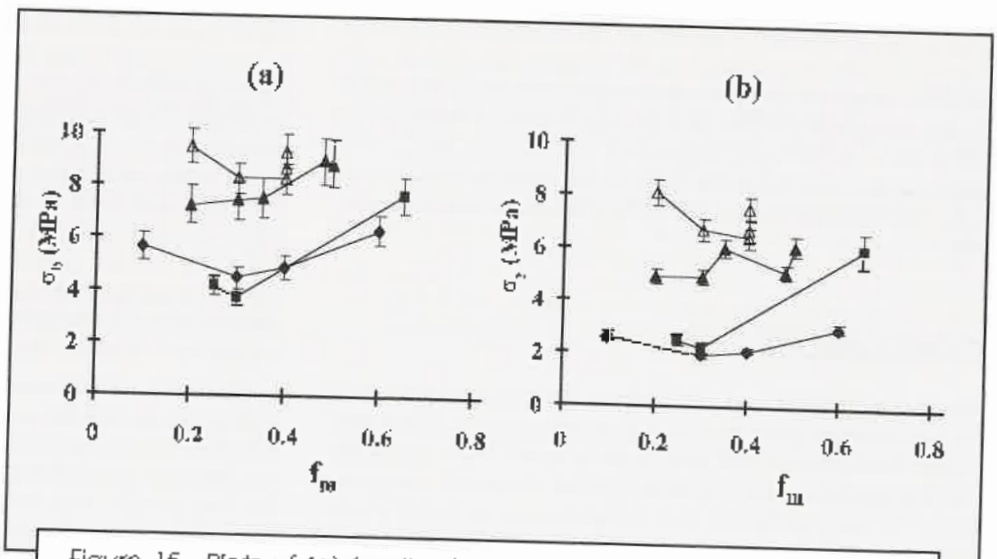


*Figure 15—Plots of (a) tensile strength ($\sigma_b$, MPa) and (b) yield stress ($\sigma_y$, MPa) vs. extent of interdiffusion $f_m$ for different types of latex films: (◆) uncrosslinked latex; (■) core-crosslinked (12%) latex; (▲) core-crosslinked (50%) latex; and (Δ) fully crosslinked latex.*

(ca. 10 MPa), dips somewhat as the films are annealed, and then increases significantly for $f_m$ greater than 0.6. The core-crosslinked (50%) and fully crosslinked latex give tougher films without annealing ($W_b \approx 16$ to 18 MPa), and the toughness does not increase very much with annealing, even though $f_m$ increases from an initial value of 0.2 to a limiting value close to 0.5. In *Figure* 13b we see the same data plotted as a function of annealing time. Here the data for the third-stage crosslinked films are included. The data are more difficult to interpret, although it is clear that extensive annealing leads to an increase in toughness for some of the samples.

A more interesting insight into the special properties of the third-stage-crosslinked latex films is provided by the data on elongation-to-break presented in *Figure* 14. As one might expect, the films prepared from uncrosslinked latex show the greatest elongation at break, nearly 400%; and films of the fully crosslinked latex exhibit the smallest strain at break (200%). The core-crosslinked (50%) latex forms films with a behavior similar to that of the fully crosslinked latex. In contrast the third-stage-crosslinked (50%) latex forms films that have strain-at-break behavior almost identical to the films formed from the latex in which the crosslinked core comprises only a small fraction (12%) of the particle volume. It is remarkable that films formed from these latex particles exhibit high elasticity at low strain rates in the oscillatory shear experiments, facile film formation, and high elongation to break that persists even upon prolonged annealing.

Values of the tensile strength $\sigma_b$ and the yield stress $\sigma_y$ as a function of $f_m$ for different film morphologies are plotted in *Figure* 15. The films prepared from uncrosslinked latex and from core-crosslinked (12%) latex have lower values of $\sigma_y$ and $\sigma_b$ for films of the $C_{x\%}S$ sample appears to increase with long annealing. For the other samples, the stress-at-break does not change much with annealing leading to increased polymer interdiffusion. Films prepared from the core-crosslinked (50%) and fully crosslinked latex have a higher tensile strength and yield stress than the other two samples shown in *Figure* 15. For these samples, the magnitude of $\sigma_b$ is only slightly larger than $\sigma_y$. As a comparison, $\sigma_b$ is $7 \pm 1$ MPa in the unannealed film of $CS_x$, and evolves to $8.2 \pm 0.4$ MPa after prolonged annealing (119 hr) at 80°C. The yield stress $\sigma_y$ is $3.8 \pm 0.3$ MPa in the unannealed film of $CS_x$ and evolves to $4.6 \pm 0.1$ MPa after prolonged annealing.

## CONCLUSIONS

We have carried out oscillatory dynamic mechanical measurements and tensile measurements on films prepared from structured and unstructured latex particles. All the particles had the same global chemical composition. The base polymer was a copolymer of butyl methacrylate and butyl acrylate with a $T_g$ of 20°C. Structure was introduced in the form of a low level (1 mol%) of crosslinking, using seeded semi-continuous emulsion polymerization to control the locus of the crosslinking agent in the particles. Most of the samples were also labeled with donor or acceptor dyes so that energy transfer experiments could be carried out. In this way we could monitor the extent of interdiffusion that occurred in each of the latex films as a function of annealing history. These ET experiments proved to be particularly useful for determining particle morphology for core-crosslinked particles in which only the core was labeled.

The linear dynamic mechanical measurements showed that $G'$ and $G''$ were sensitive to the particle morphology, with particular sensitivity exhibited by the elastic modulus $G'$. The tensile properties were less sensitive to particle morphology. Films for tensile experiments were substantially thicker (0.8 mm) than those commonly used for ET studies of polymer diffusion in latex films. Film thickness has no effect on the polymer diffusion rate, but the films for tensile testing were subjected to prolonged drying at 39°C. Under these conditions, sufficient polymer interdiffusion occurs during film formation for the films to acquire substantial strength and toughness. Some differences due to morphology are apparent. Films formed from fully crosslinked latex and from core-crosslinked latex with a large core fraction (50 vol%) have somewhat larger tensile strengths, yield strengths, and toughness than those formed from uncrosslinked latex or latex with a small (12%) crosslinked core. These differences become less pronounced when the samples are annealed for long periods of time (100+ hr) at 80°C.

Some of the most interesting results were obtained on films prepared from third-stage-crosslinked latex. These films exhibit unusual dynamic mechanical properties, with high elasticity at low shear rates. The system forms tough elastic films with a large elongation at break, nearly 350%. The latexes themselves are unlikely to have a core-shell morphology with a crosslinked shell. Rather, we anticipate a semi-interpenetrating network-like structure in which the uncrosslinked component is free to diffuse across the intercellular boundaries in the latex film. This is a system which merits further attention in future experiments.

We would like to emphasize that our results for the films formed from the fully crosslinked latex are very different than those reported by Zosel and Ley[7,29] for films of PBMA copolymer latex crosslinked with 2 mol% methallyl methacrylate. Their films, which have a $T_g$ somewhat above room temperature (ca. 30 C), are brittle, even when annealed extensively at 90°C. They exhibit no yield and have a tensile strength close to zero. They have argued that the crossover from tough to brittle behavior occurs when the mean molecular weight between crosslinks $M_c$ becomes smaller than the entanglement molecular weight $M_e$, determined from the plateau modulus of the corresponding linear polymer.

Recently de Gennes and his co-workers[30,31] have developed a model for adhesion between crosslinked elastomers. The model focuses on the role of connector molecules such as the dangling ends of crosslinked network. In this model, the energy of crack propagation is opposed by the work necessary to overcome the frictional resistance to pull-out of the connector chains. For connector molecules that traverse the interface several times, this work can be greater than that necessary to break a backbone bond in the connector chain.[31] The authors

comment that in glassy polymers, chain cleavage may occur in preference to chain pull-out. While this model does not explain the change in behavior found by Zosel and Ley for PBMA networks when $M_c$ becomes less than $M_e$, it does suggest that the difference between our results and theirs may be due to a difference in glass transition temperature as well as a difference in crosslink density. Results which support the importance of $T_g$ on the behavior of adhesion in latex films prepared from crosslinked particles is provided by the recent publication of Tamai et al.[32]

## ACKNOWLEDGMENTS

The authors thank Elf-Atochem and NSERC Canada for their support of this research.

### References

(1) Voyutskii, S.S., *Autohesion and Adhesion of High Polymers*, Wiley-Interscience, New York, 1963.

(2) Vanderhoff, J.W., "Mechanism of Film Formation of Latexes," *Br. Polym. J.*, 2, 161 (1970).

(3) Linne, M.A., Klein, A., Miller, G., and Sperling, L.S., "Film Formation from Latex: Hindered Initial Interdiffusion of Constrained Polystyrene Chains Characterized by Small-Angle Neutron Scattering," *J. Macromol. Sci. Phys.*, *B27*, 217-231 (1988).

(4) Ahagon, A. and Gent, A., "Effect of Interfacial Bonding on the Strength of Adhesion," *J. Polym. Sci., Polym. Phys. Ed.*, *13*, 1285-1300 (1995).

(5) Mohammed, S., Daniels, E.S., Sperling, L.H., Klein, A., and El-Aasser, M.S., "Isocyanate-Functionalized Latexes: Film Formation and Tensile Properties," *J. Appl. Polym. Sci.*, *66*, 1869 (1997).

(6) Feng, J., Pham, H., Macdonald, P., Winnik, M.A., Guerts, J., Zirkel, H., van Es, S., and German, A.L., "Formation and Crosslinking of Latex Films through the Reaction of Acetoacetoxy Groups with Diamines Under Ambient Conditions," JOURNAL OF COATINGS TECHNOLOGY, *70*, No. 881, 57 (1998).

(7) Zosel, A. and Ley, G., "Influence of Crosslinking on Structure, Mechanical Properties, and Strength of Latex Films," *Macromolecules*, *26*, 2222-2227 (1993).

(8) (a) Zhao, C.-L., Wang, Y., Hruska, Z., and Winnik, M.A., "Molecular Aspects of Latex Film Formation: An Energy-Transfer Study," *Macromolecules*, *23*, 4082-4087 (1990); (b) Wang, Y., Zhou, C-L., and Winnik, M.A., "Molecular Diffusion and Latex Film Formation: An Analysis of Direct Nonradiative Energy Transfer Experiments," *J. Chem. Phys.*, *95*, 2143-2153 (1991).

(9) (a) Winnik, M.A., Wang, Y., and Haley, F., "Latex Film Formation at the Molecular Level: The Effect of Coalescing Aids on Polymer Diffusion," JOURNAL OF COATINGS TECHNOLOGY, *64*, No. 811, 51 (1992); (b) Feng, J. and Winnik, M.A., "Effect of Water on Polymer Diffusion in Latex Films," *Macromolecules*, *30*, 4324-4331 (1997).

(10) Dhinojwala, A. and Torkelson, J.M., "A Reconsideration of the Measurement of Polymer Interdiffusion by Fluorescence Nonradiative Energy Transfer," *Macromolecules*, *27*, 4817-4824 (1994).

(11) Richard, J., "Dynamic Micromechanical Properties of Styrene-Butadiene Copolymer Latex Films," *Polymer*, *33*, 3, 562-572 (1992).

(12) Cavaillé, J.Y., Jourdan, C., Kong, X.Z., Perez, J., Pichot, C., and Guillot, J. "Comparison of Micromechanical Properties of Latex Films Obtained by Different Emulsion Copolymerization Pathways," *Polymer*, *27*, 691 (1986).

(13) Feng, J., "Molecular and Environmental Aspects of Latex Film Formation," Ph.D. Thesis, University of Toronto, 1996.

(14) Sosnowski, S., Feng, J., and Winnik, M.A., "Dye Distribution in Fluorescent-Labeled Latex Prepared by Emulsion Polymerization," *J. Polym. Sci., Chem. Ed.*, *32*, 1497-1505, (1994).

(15) O'Connor, D. and Phillips, D., *Single Photon Counting*, Academic Press, New York, 1984.

(16) (a) Kim, H.-B., Wang, Y., and Winnik, M.A., "Synthesis, Structure and Film-Forming Properties of Poly(butyl methacrylate)-Poly(methacrylic acid) Core-Shell Latex," *Polymer*, *35*, 1779-1786 (1994); (b) Liu, Y. S., Feng, J., and Winnik, M.A., "Study of Polymer Diffusion Across the Interface in Latex Films Through Direct Energy Transfer Experiments," *J. Chem. Phys.*, *101*, 9096-9103 (1994).

(17) Ferry, J.D., *Viscoelastic Properties of Polymers*, 3rd Ed., Chap. 11, Wiley, New York, 1980.

(18) Birks, J.B., *Photophysics of Aromatic Molecules*, Wiley, New York, 1970.

(19) Berlman, I.B., *Energy Transfer Parameters of Aromatic Molecules*, Academic Press, New York, 1973.

(20) Lakowicz, J.R., *Principles of Fluorescence Spectroscopy*, Plenum Press, New York, 1983.

(21) While the synthesis of An-labeled latex was successful here, the use of this monomer in other systems containing a higher ratio of acrylate/methacrylate has led to inhibition of polymerization. This is a serious problem if one wishes to use EI techniques to study polymer diffusion in acrylate-rich latex films. A new anthracene-containing monomer has been developed which is suitable for acrylate polymerization. Liu, R. and Winnik, M.A., unpublished results.

(22) Feng J., Winnik, M.A., and Siemiarczuk, A., "Interface Characterization in Latex Blend Films by Fluorescence Energy Transfer," *J. Polym. Sci, Part B: Polym. Phys.*, *36*, 1115-1128 (1998).

(23) Zosel, A., "Mechanical Properties of Films from Polymer Latex," *Polym. Adv. Technol.*, *6*, 263 (1995).

(24) Treolar, L.R.G., *The Physics of Rubber Elasticity*, Clarendon Press, Oxford, U.K., 1958.

(25) Winter, H.H. and Chambon, F., "Analysis of the Linear Viscoelasticity of a Crosslinking Polymer at the Gel Point," *J. Rheol.*, *30*, 367 (1986).

(26) Scanlan, J.C. and Winter, H.H., "Composition Dependence of the Viscoelasticity of End-Linked Poly(dimethylsiloxane) at the Gel Point," *Macromolecules*, *24*, 47 (1991).

(27) Lambla, M., Schlund, B., Tazarus, F., and Pith, T., "Effects of Reaction Pathway in Emulsion Copolymerization on Film Mechanical Properties," *Makromol. Chem. Suppl.*, *10/11*, 463-476 (1985).

(28) Cavaillé, J.-Y., Vassoille, R., Tholet, G., Rios, L., and Pichot, C. "Structural Morphology of Polystyrene-poly(butyl acrylate) polymer-polymer Composites Studies by Dynamic Mechanical Measurements," *Colloid Polym. Sci.*, *269*, 248-258 (1991).

(29) Zosel, A. and Ley, C., "Film Formation of Latices with Crosslinked Particles," *Polym. Bull.*, *27*, 459-464 (1992).

(30) Raphael, E. and de Gennes, P.G., "Rubber Rubber Adhesion with Connector Molecules," *J. Phys. Chem.*, *96*, 4002-4007 (1992).

(31) Ji, H. and de Gennes, P.G., "Adhesion via Connector Molecules: The Many-Stitch Problem," *Macromolecules*, *26*, 520-525 (1993).

(32) Tamai, T., Pineri, P., and Winnik, M.A., "Effect of Crosslinking on Polymer Diffusion in Poly(butyl methacrylate-co-butyl acrylate) Latex Films, I," *Macromolecules*, *32*, 6102-6110 (1999).